

2018

Post-Earthquake Structural Damage Assessment Through Point Cloud Data

Mohammad Ebrahim Mohammadi
University of Nebraska-Lincoln, me.m@huskers.unl.edu

Richard L. Wood
University of Nebraska-Lincoln, rwood@unl.edu

Follow this and additional works at: <https://digitalcommons.unl.edu/civilengfacpub>

 Part of the [Civil Engineering Commons](#), and the [Structural Engineering Commons](#)

Mohammadi, Mohammad Ebrahim and Wood, Richard L., "Post-Earthquake Structural Damage Assessment Through Point Cloud Data" (2018). *Civil Engineering Faculty Publications*. 161.
<https://digitalcommons.unl.edu/civilengfacpub/161>

This Article is brought to you for free and open access by the Civil Engineering at DigitalCommons@University of Nebraska - Lincoln. It has been accepted for inclusion in Civil Engineering Faculty Publications by an authorized administrator of DigitalCommons@University of Nebraska - Lincoln.



Eleventh U.S. National Conference on Earthquake Engineering
Integrating Science, Engineering & Policy
June 25-29, 2018
Los Angeles, California

POST-EARTHQUAKE STRUCTURAL DAMAGE ASSESSMENT THROUGH POINT CLOUD DATA

M. E. Mohammadi¹ and R. L. Wood²

ABSTRACT

Structural damage assessment following an extreme event can provide valuable information and insight into unanticipated damage and failure modes to improve design philosophies and design codes as well as reduce vulnerability. Oftentimes, structural engineers create finite element models (FEM) of the structure in which numerous model parameters require calibration to simulate the current state. This information may include structural plan details (geometry), material characteristics (strength and stiffness parameters), as well as observed damage patterns (cracks, spalling, etc.). Ground-based lidar (GBL) scans and Structure-from-Motion (SfM) can rapidly capture dimensionally accurate point clouds of the structure or facility of interest. Furthermore, point clouds can be used to efficiently document perishable structural damage data digitally prior to recovery or retrofit efforts. Within these point clouds, information can be extracted to objectively locate damage patterns in non-temporal datasets. Localization and quantification of damage can serve to update models with high fidelity within forensic investigations as well as to estimate the remaining structural capacity. In this work, an algorithm based on two spatially invariant geometrical features was used to identify and quantify structural damage from point cloud data for two case study buildings. The first case-study building is an 18-story high-rise condominium building that was significantly damaged during the 2015 Gorkha (Nepal) Earthquake. The damage included significant cracks in partition walls, unreinforced masonry infill walls, and section-loss within coupling beams and staircases at various levels. The second case-study structure, from the same earthquake event, is a five-tiered pagoda style temple built using timber beams and thick brick masonry walls. The temple sustained moderate damage where shear cracks developed at lower levels and seams of the wall piers. Through the developed damage detection method, cracking, concrete spalling, and loss of cross section within the point cloud data of the nonstructural and structural elements are quantified.

¹Graduate Student Researcher, Dept. of Civil Engineering, University of Nebraska-Lincoln, Lincoln, NE 68503

²Assistant Professor, Dept. of Civil Engineering, University of Nebraska-Lincoln, Lincoln, NE 68503

POST-EARTHQUAKE STRUCTURAL DAMAGE ASSESSMENT THROUGH POINT CLOUD DATA

M. E. Mohammadi¹ and R. L. Wood²

ABSTRACT

Structural damage assessment following an extreme event can provide valuable information and insight into unanticipated damage and failure modes to improve design philosophies and design codes as well as reduce vulnerability. Oftentimes, structural engineers create finite element models (FEM) of the structure in which numerous model parameters require calibration to simulate the current state. This information may include structural plan details (geometry), material characteristics (strength and stiffness parameters), as well as observed damage patterns (cracks, spalling, etc.). Ground-based lidar (GBL) scans and Structure-from-Motion (SfM) can rapidly capture dimensionally accurate point clouds of the structure or facility of interest. Furthermore, point clouds can be used to efficiently document perishable structural damage data digitally prior to recovery or retrofit efforts. Within these point clouds, information can be extracted to objectively locate damage patterns in non-temporal datasets. Localization and quantification of damage can serve to update models with high fidelity within forensic investigations as well as to estimate the remaining structural capacity. In this work, an algorithm based on two spatially invariant geometrical features was used to identify and quantify structural damage from point cloud data for two case study buildings. The first case-study building is an 18-story high-rise condominium building that was significantly damaged during the 2015 Gorkha (Nepal) Earthquake. The damage included significant cracks in partition walls, unreinforced masonry infill walls, and section-loss within coupling beams and staircases at various levels. The second case-study structure, from the same earthquake event, is a five-tiered pagoda style temple built using timber beams and thick brick masonry walls. The temple sustained moderate damage where shear cracks developed at lower levels and seams of the wall piers. Through the developed damage detection method, cracking, concrete spalling, and loss of cross section within the point cloud data of the nonstructural and structural elements are quantified.

¹Graduate Student Researcher, Dept. of Civil Engineering, University of Nebraska-Lincoln, Lincoln, NE 68503 (email: me.m@huskers.unl.edu)

²Assistant Professor, Dept. of Civil Engineering, University of Nebraska-Lincoln, Lincoln, NE 68503 (email: rwood@unl.edu)

Introduction

Digital technology to create point cloud data from real-world environments have been evolved in recent decades and enable users to collect data efficiently. Point clouds, a set of vertices in the three-dimensional space that represents the surface of objects, can be created with various methods including light detection and ranging technology (lidar) or a computer vision method known as Structure-from-Motion (SfM). Lidar systems (i.e., ground based lidar or GBL) generate geometrically accurate point cloud data which have been implemented within civil engineering applications including laboratory testing to measure displacement data [1, 2], documenting scene for forensic investigation scenarios [3], preserving damaged structures after an extreme event prior cleanup operations (e.g., earthquake) [3, 4, 5], exporting accurate dimensions and geometry form objects of interest for structural engineering purposes [6], and further analyze the point cloud data and their corresponding color information data (i.e., images captured by lidar platform) or intensity field data to detect surface defects, cracks, or volumetric losses [7, 8, 9, 10, 11, 12]. SfM-derived point clouds are formed from a set of images collected from the object or region of interest. As a result, SfM-derived point clouds inherently lack real-world dimensions and accuracy can verify as a function of ground control (e.g., georeferencing). Although SfM-derived point cloud formation requires a longer process, data collection can rapid and efficient using unmanned aerial systems (UAS) with an onboard camera of large civil structures and networks. The potential of UAS SfM-derived point clouds in characterizing structural damage of built up areas after 2015 Gorkha earthquake and geotechnical reconnaissance after M_w 7.8 Iquique 2014 Chile earthquake has been proven the utility of UAS for data collection after an extreme event [13, 14, 15]. While SfM-derived data can be used as source for estimating the damage to urban areas, decision making processes, and landslide quantifications of large areas, due to variation in accuracy and density, it may be less reliable for detailed structural assessment in comparison with GBL.

The focus of this manuscript is to analyze the lidar-derived point cloud data for structural damage detection and localization. To achieve this objective, structural and nonstructural member point clouds of two structures with simple to complex geometries, damaged during 2015 Gorkha earthquake, were analyzed as evaluation data. These datasets were analyzed based on the spatial orientation of each point with respect to their local neighboring points to identify surface defects, cracks and spalling [11, 12].

Methodology

Detecting structural damage through point cloud data had been explored by previous researchers. For example, Olsen et al. [7] and Kashani et al. [16] investigated damage characterization through intensity values. Kim et al. [8] introduced a method to assess point cloud data of only flat surface. Valenca et al. [9] and Erkal and Hajjar [10] evaluated the variation of surface geometry and color information data to identify defects. More recently, Hou et al. [17] has tested various clustering algorithms to analyze the point cloud data based on color information for surface defects. Although successful in detecting defects, these methods have a few limitations in terms of applicability (i.e. can only analyze planar surfaces) dependency to lighting and environmental conditions (i.e., vulnerability to presence darker areas due to moisture), or long preprocessing steps (e.g., intensity correction [18]). Furthermore, Olsen [19] developed a method to detect temporal changes within a point cloud data of multiple elements using change detection through a point cloud comparison collected at two distinct states. Although the method can be accurate and reliable in detecting

changes (including structural damage), it requires a baseline or reference point cloud for comparison which limits its application to the sites that a reliable reference scan is available.

Within this work, to identify surface defects, cracks, and volumetric losses, the variation of each point with reference to its local closest neighboring points are investigated through two independent spatially invariant surface feature descriptors [11,12]. The implemented method relies solely on spatial variation of points computed by the two features. This method does not require a baseline or color information as a reference or compliment dataset, respectively. To analyze the point cloud, initially the input dataset is preprocessed to reduce erroneous points. Then, the processing step is concluded by regularizing the point-to-point spacing within the dataset to ameliorate the variation of point density. Afterwards, the variation of each point with respect to their selected number of closest neighboring vertices are evaluated through two surface feature descriptors. The first surface descriptor is known as surface variation, which is computed based ratio of smallest to total summation of eigenvalue of covariance matrix of each point and its neighboring vertices. The second surface descriptor is the variation of each point normal vector with respect to a local reference plane. To compute normal vector for each point, a weighted average of the normal vector of adjacent triangles of selected neighboring vertices is used [20], and the local reference plane is identified over a larger neighborhood of vertices through computing the best fitted least square plane [21]. Once both surface feature descriptor values are computed, a probability distribution function (pdf) for each feature is identified using a Kernel pdf [22]. Then the vertices are classified into two groups of likely damage and undamaged based on selected confidence level percentile. In the final step, the algorithm compares each feature's classification result and update the classification of each point if and only if it was classified as damage by both features.

The described damage detection algorithm only requires five input parameters to identify likely damage points. This include the point-to-point regulating step size, number of neighboring vertices for surface variation, computation of point normal vector, and local reference plane for each point, as well as the damaged confidence level. As the point-to-point regulating step uniforms the point-to-point spacing within the cloud, it directly influences the damage detection accuracy. Therefore, it should to be selected based on the desired dimension of the damage that are of interest. In addition, the overall density of the cloud should also be considered in selection of point-to-point spacing, as very small or large grid steps will not result in point cloud with uniform density and may limit the detectability of the developed method. For this study, based on the dataset densities and desired level of detection, clouds were regulated between 0.5 to 1.25 cm grid steps. The second, third and fourth parameters selected are number of closest neighboring points. Multiple runs on various datasets demonstrated that evaluating the described surface feature descriptors and local reference planes for 8 and 24 number closet neighboring points, respectively, can readily capture and reveal the surface variation. The last input parameter is related to damage confidence level, which is an initial guess of percent damage of input dataset.

Application of the Described Method on After 2015 Gorkha Earthquake

On April 24, 2015, a M_w 7.8 earthquake shook the Gorkha district of central Nepal (~80 km northwest of Kathmandu) at the focal depth of 15k m [23,24]. The main event was followed by a series of aftershocks up to a M_w of 7.3 resulting in significant damage to both historic and urbanized areas of the country. After a few months from the event, a group of researchers from various universities visited the affected areas and documented the buildings performance and

damage during the event [25]. To evaluate the performance of the developed method in detecting defects, cracks and other surface nonuniformities, two case study structures have been selected from those visited structures that were moderately damaged. Each selected structure represents a different construction method, material, and geometry. The first structure selected is an 18-story reinforced concrete (RC) apartment building located in Hattiban, Katmandu, approximately 80 km southeast of main shock epicenter. The second case study structure was an historic five-tiered pagoda styled temple initially built in 1702 with unreinforced brick masonry with mud-mortar. The temple had a height of approximately 22 m and was in the Bhaktapur, in the Katmandu Valley, approximately 100 km southeast of main shock epicenter.

18-story Reinforced Concrete Building

The 18-story RC apartment building sustained moderate damage as result of the main event and the following aftershocks. The damage observed in various components including nonstructural exterior and interior infill walls, separation of infill walls and adjacent columns, beam-column joint cracking, and concrete spalling and cracking within the coupling beam elements. To document the sustained damage throughout the structure the team utilized Faro Focus X-130 scanner. A phased-based scanner, Faro X-130 can collect up to 1 million points per second at range of 130 meters [26]. A total of 16 lidar scans were collected from 5 selected levels, namely the 3rd, 6th, 9th, 12th, and 15th floors. This pattern of data, allows to document damage throughout the structure and study the damage propagation and evolution as the function of building height. To achieve this objective, two common members were selected and analyzed by the damage detection method. Fig. 1a represents the typical scanner setup for each floor to scan the common members throughout the structure [11]. The first member selected was a 1.7 m long coupling beam located roughly at the center of structure (Fig 1b). The second member was a 4 m by 2.7 m (L×H) infill interior wall located at the west of the structure (Fig. 1c).

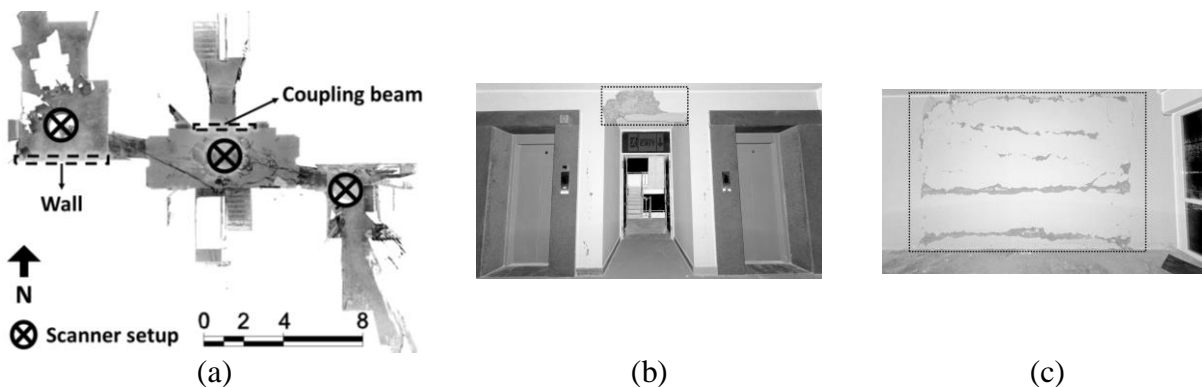


Figure 1. 18-story structure damage survey: (a) top view of floor along with typical scan placements and location of common members to investigate the damage Evolution. (b) View of coupling beam and (c) view of the interior masonry infill wall [11].

The coupling beam point cloud consists of two surfaces of beam as demonstrated in Fig. 2a. This will allow to assess the performance of the developed method for data with more complex geometries, here a coplanar surface. The analysis result of the coupling beam is illustrated in Fig. 2b. To analyze this cloud, initially the point-to-point spacing was regulated to 0.5 cm. Afterwards, the two geometrical features for each point and its 8 closet neighboring points were computed and

initial damage confidence level was set to 60%. Then, the developed method identified the significant concrete spalling and exposed rebars within the point cloud. Fig. 2b illustrates the results of the methodology. The output damage percentile after damage evaluation step was 47%. The second selected point cloud from this high-rise building is the common wall, which is a planar surface. As shown in Fig 3a, the common wall sustained significant horizontal cracking in the middle and its perimeter where it meets the beam and columns. To analyze the wall, initially the point-to-point spacing was regulated to 0.5 cm. Then, the significant cracking and other defects were identified through comparison of each surface feature and initial damage confidence level of 50% (Fig. 3b). The final damage percentile for the wall was 11%.

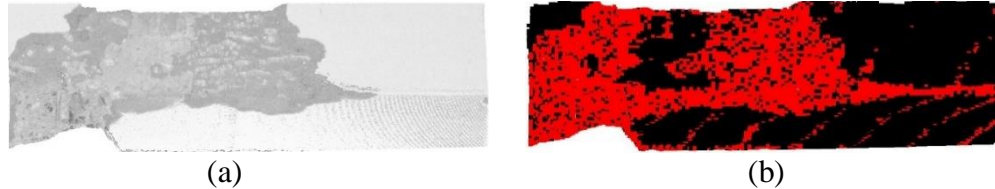


Figure 2. Evaluation of detected damage for the coupling beam: (a) black and white point cloud of the beam (b) color-coded point cloud where detected surface defects are shown in red (grey) [11].

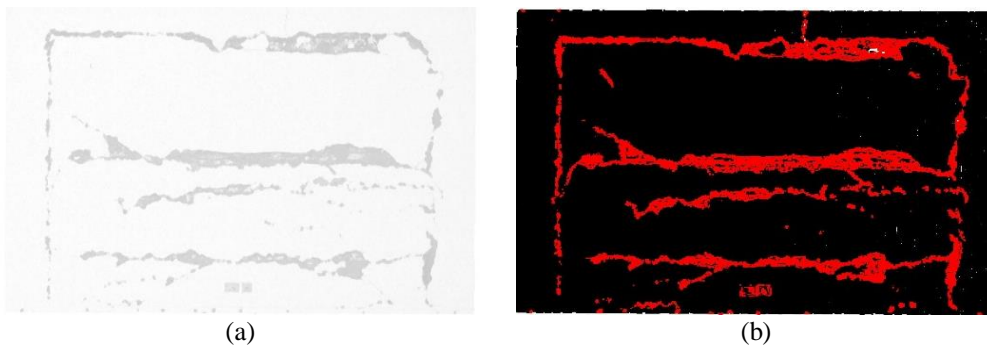


Figure 3. Evaluation of detected damage for the selected wall: (a) black and white point cloud of the wall and (b) color-coded point cloud where the detected surface defects are shown in red (grey) [11].

Damage Analysis of Pagoda Style Temple Masonry Walls

The second structure selected is the Nyatapola Temple which sustained moderate-to-severe damage during the earthquake sequence. A series of large shear cracks were observed at the base level exterior walls, in close proximity to door frames, as well as various surface defects including loss of grout and dislodged bricks throughout the structure. To survey the structure, the research team performed a total of 38 scans at various distances [27]. Fig. 4a represents the final point cloud of the Nyatapola temple. Due to various activities during the scanning sequence at the base level, architectural design of the temple, and to minimize the occlusion in the final point cloud data, a total of 26 of those 38 scans were conducted at the base level to the bottom of the tiered plinth (Fig. 4b). To evaluate the developed method for the earthen masonry wall, a single scan of the base level north wall was used as input data which contains approximately 9 million points (Fig. 5a). The location of the selected scan is highlighted in Fig. 4b. As a result, the point cloud contains various damage patterns (e.g. crack at the north wall) and occlusion due to the presence of ornate

architecture.

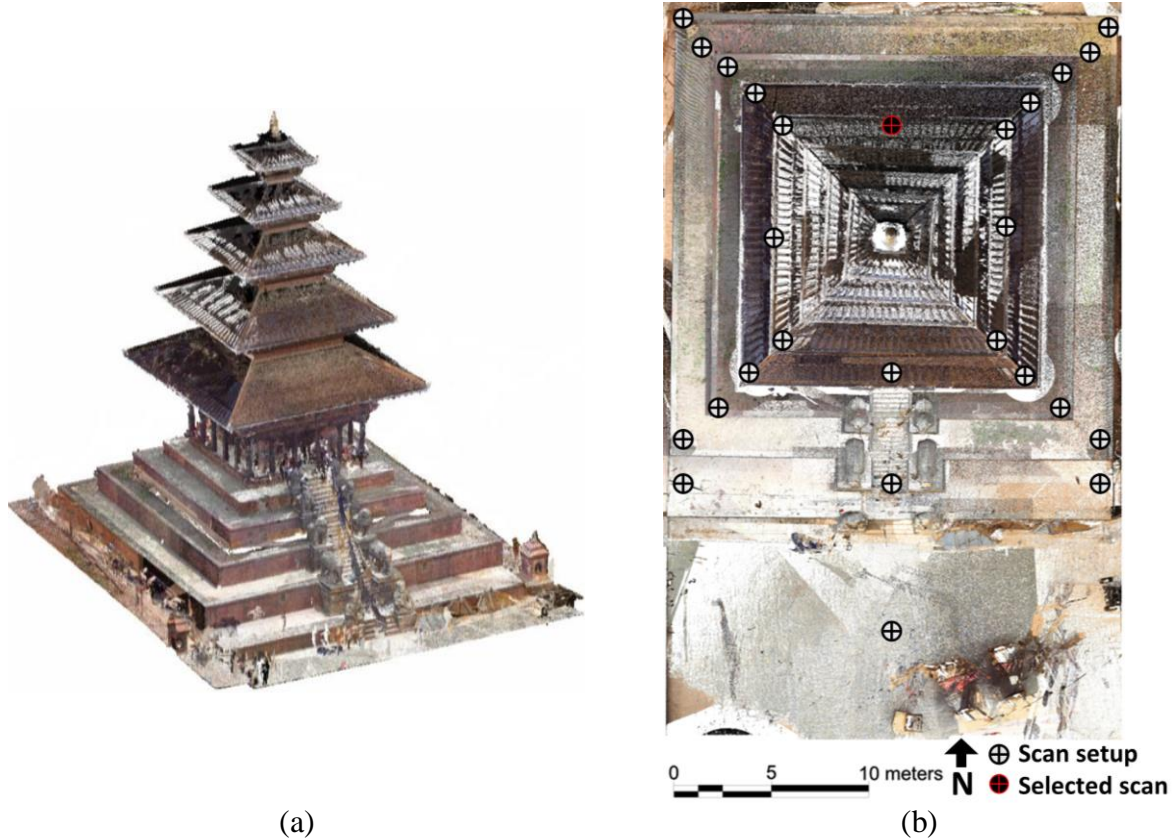


Figure 4. Nyatapola temple structure: (a) southwest isometric view and (b) plan view of scan locations along with the location of selected scan [27].

To analyze the five-story temple, the point cloud was first regulated to a point spacing of 1.25 cm. This is larger than the high-rise structure due to the large variation in point density near corners as a result of laser beam dispersion and due to the close scanner placement to the structure with a resultant high angle of attack at the corners. Then, the two geometrical features were computed for each vertex and its 8 closet neighbors. Also, the initial damage confidence level was set to 60%. Following the damage evaluation step, Fig. 5b illustrates the result of each feature classification and the identified significant cracks and other surface defects. The developed method was able to detect all surface defects and cracks with dimensions of 1.25 cm and larger. This includes the large shear crack on the top right of the entrance. Furthermore, this developed method was successful in the identification of damage near the two edges despite the occlusions in the point cloud. One drawback however, the method falsely identified a series of point as likely damage due to the ornate architectural details of the wall sculptures and door lintel. Using these results, the detected damage enabled analysts to measure the defects with a high-level confidence to characterize the structure and update a finite element model [27]. The quantification results for the significant crack on the top right of the entrance (crack C1) are presented in Table 1. To measure the crack length, the total length of the highlighted connected segments in the horizontal direction was measured. Similarly, to measure the width of the crack, multiple measurements in the vertical direction were taken and the mean width is reported.

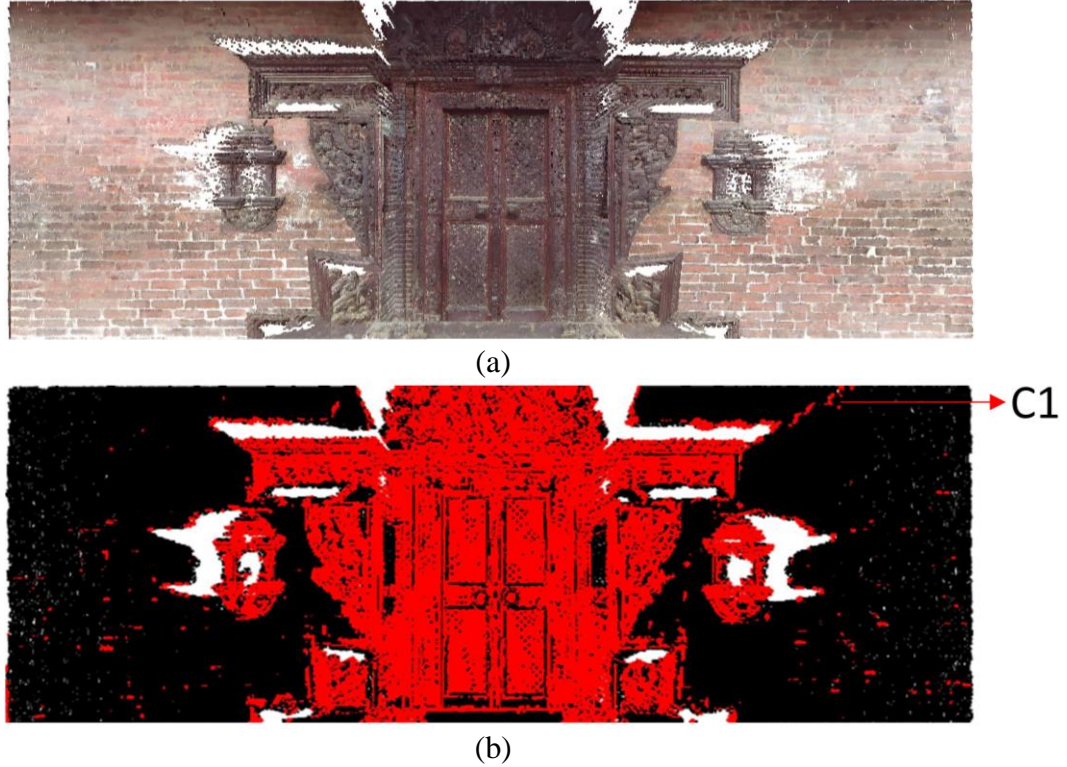


Figure 5. North wall damage detection details: (a) RGB colored point cloud and (b) color coded point cloud where the detected surface defects are shown in red (grey).

Table 1. Details of detected cracks from the first-floor exterior wall.

Classification	Quantified Damage
Shear crack western side of door frame	68 cm (L) by .3.25 cm (W)

Conclusions

This manuscript presents a newly developed approach to detect objectively likely surface defects from the point clouds for two case study structures [12]. The first case study structure consists of two segmented point clouds with planar (wall) and co-planar (coupling beam) geometries. The method was able to detect the major cracks, spalling, cross-loss section, and exposed rebars within the both point clouds. The second cases study represents an earthen masonry wall constructed with mud-mortar and contained ornate architectural details at the wall and door frame. As a result, the point cloud of the second case study introduced even more complex surface geometry, particularly at the local level due to the irregularities in the brick and mortar. Furthermore, the analysis of the temple highlighted the method's robustness for uneven point density and occlusion, while maintaining its sensitivity to detect surface defects including cracks, loss of grout, and dislodged bricks. However, the shadow effects due to occlusion and presence of sharp features (e.g., ornate sculptures) can lead to false positives which can be reduced in future work.

Acknowledgments

University of Nebraska Foundation provided financial support for data collection following the event. In addition, the authors would like to appreciate the collaborators in Oregon State University (OSU), University at Buffalo (UB), Tufts University, local building owners/managers (for 18-story structure), and Bahktapur Municipality (for the Nyatapola Temple) who aided site access. Special individuals included Dr. Andre Barbosa (OSU), Mr. Supratik Bose (UB), Mr. Rajendra Soti (OSU), and Mr. Sandip Timsina (formerly UNL), Mr. Patrick Burns (OSU), Dr. Matthew Gillins (OSU), and Dr. Matthew O'Banion (OSU) for their assistance in the field collection of data. The opinions, findings, and conclusions expressed in this paper are those of the authors and do not necessarily reflect those of sponsoring units, organizations, and collaborators involved in this project.

References

1. Park, HS, Lee, HM, Adeli, H, Lee. A new approach for health monitoring of structures: terrestrial laser scanning. *Computer-Aided Civil and Infrastructure Engineering* 2007; **22** (1): 19-30.
2. McMullin, KM, Takhirov, S, Gunay, S, Yarra, S, Tai, E. Scanner and digital displacement technology for documentation of experimental building façade test specimens. *Proceedings of the 10th National Conference in Earthquake Engineering*, Earthquake Engineering Research Institute, Anchorage, AK, 2014.
3. Kayen R, Olsen MJ. Post-earthquake and tsunami 3D laser scanning forensic investigations. *Journal of Forensic Engineering* 2012; 2012, pp.477-486.
4. Mosalam KM, Takhirov SM, Park, S. Applications of laser scanning to structures in laboratory tests and field surveys. *Structural Control and Health Monitoring* 2014; **21** (1): 115-134.
5. Bose S, Nozari A, Mohammadi ME, Stavridis A, Babak M, Wood R, Gillins D, Barbosa A. Structural assessment of a school building in Sankhu, Nepal damaged due to torsional response during the 2015 Gorkha earthquake. *Proceedings of the Society for Experimental Mechanics Series*, Orlando, FL, 2016; Volume 2: 31-41.
6. Wittich CE, Hutchinson TC, Wood RL, Seracini M, Kuester F. Characterization of Full-Scale, Human-Form, Culturally Important Statues: Case Study. *Journal of Computing in Civil Engineering* 2016; 05015001.
7. Olsen, MJ, Kuester, F, Chang, BJ, Hutchinson, TC. Terrestrial laser scanning-based structural damage assessment. *Journal of Computing in Civil Engineering* 2009; **24** (3): 264-272.
8. Kim, MK, Sohn H., Chang., CC. Localization and quantification of concrete spalling defects using terrestrial laser scanning. *Journal of Computing in Civil Engineering* 2014; **29** (6): 04014086.
9. Valença, J, Puente, I, Júlio, E, González-Jorge, H, Arias-Sánchez, P. Assessment of cracks on concrete bridges using image processing supported by laser scanning survey. *Journal of Construction Build Materials* 2017; 146: 668-678.
10. Erkal, BG, Hajjar, JF. Laser-based surface damage detection and quantification using predicted surface properties. *Automation in Construction* 2017; 83: 285-302.
11. Yu, H, Mohammed, MA, Mohammadi, ME, Moaveni, B, Barbosa, AR, Stavridis, A, Wood, RL. Structural identification of an 18-Story RC building in Nepal using post-earthquake ambient vibration and lidar data. *Frontiers Built Environment* 2017; 3: 11.
12. Mohammadi, ME, Wood, RL. Identification of key geometrical features for automatic structural damage detection from point clouds. *Proceedings in International Workshop on Structural Health Monitoring*, Stanford, CA, 2017.
13. Moss, RE, Thompson, EM, Kieffer, DS, Tiwari, B, Hashash, YM, Acharya, I, Dahal, S. Geotechnical effects of the 2015 magnitude 7.8 Gorkha, Nepal, earthquake and aftershocks. *Seismological Research Letters* 2015; 86 (6): 1514-1523

14. Wood, RL, Gillins, DT, Mohammadi, ME, Javadnejad, F, Tahami, H, Gillins, MN, Liao, Y. 2015 Gorkha post-earthquake reconnaissance of a historic village with micro unmanned aerial systems. *Proceedings in 16th World Conference on Earthquake (16WCEE)*, Santiago, Chile, 2017.
15. Rollins K, Ledezma C, Montalva G. Geotechnical aspects of April 1, 2014, M8.2 Iquique, Chile earthquake. *Geotechnical Extreme Event Reconnaissance GEER Association*, Report no. GEER-038, San Luis Obispo, CA., USA, 2014.
16. Kashani, AG, Graettinger, AJ. Cluster-based roof covering damage detection in ground-based lidar data. *Automation in Construction* 2015; 58: 19-27.
17. Hou, TC, Liu, JW, Liu, YW. Algorithmic clustering of LiDAR point cloud data for textural damage identifications of structural elements. *Measurement* 2017; 108: 77-90.
18. Kashani, AG, Olsen MJ, Graettinger AJ. Laser scanning intensity analysis for automated building wind damage detection. *Proceedings in International Workshop on Computing in Civil Engineering*, ASCE, Austin, TX, 2015.
19. Olsen, MJ. In situ change analysis and monitoring through terrestrial laser scanning. *Journal of Computing in Civil Engineering* 2013; **29** (2): 04014040.
20. Jin, S, Lewis, RR, West, D. A comparison of algorithms for vertex normal computation. *Visual Computer* 2005; **21** (1-2): 71-82.
21. Shakarji, CM. Least-squares fitting algorithms of the NIST algorithm testing system." *Journal of Research of NIST*. 1998; 103: 633-641.
22. Shalizi, C. *Advanced data analysis from an elementary point of view*. Cambridge University Press, Cambridge, UK, 2013.
23. Rai, DC, Singhal, V, Raj, SB, Sagar, SL. Reconnaissance of the effects of the M7.8 Gorkha (Nepal) earthquake of April 25, 2015. *Geomatics, Natural Hazards and Risk* 2015; 7: 1–17.
24. Rupakhety, R. Seismotectonic and Engineering Seismological Aspects of the M w 7.8 Gorkha, Nepal, Earthquake. *In Impacts and Insights of the Gorkha Earthquake* 2018; 19-45.
25. Brando, G, Rapone, D, Spacone, E, Barbosa, A, Olsen, MJ, Gillins, D, Soti R, Varum, H, Arède, A, Vila-Pouca, N, Furtado, A, Oliveira, J, Rodrigues, H, Stavridis, A, Bose, S, Faggella M, Gigliotti R, Wood RL. Reconnaissance report on the 2015 Gorkha earthquake effects in Nepal. *Proceedings in XVI Convegno ANIDIS*. L'Aquila, Italy, 2015.
26. Faro. *Faro laser scanner focus 3D: features, benefits & technical specifications*. FARO Technologies. Lake Mary, FL, 2011.
27. Wood, RL, Mohammadi, ME, Barbosa, AR, Abdulrahman, L, Soti R, Kiran Kawan, C., Shakya, M, Olsen, MJ. Damage assessment and modeling of the five-tiered pagoda style Nyatapola temple. *Earthquake Spectra* 2017.